Binuclear gold(I) complexes with bridging diisocyanides and X-ray structures of [Au(ᵗBuNC)(CN)], [Au_2(dmb)$(CN)_2$] and [Au_2(tmb)$(CN)_2$] (tmb = 2,5-diisocyano-2,5-dimethylhexane; dmb = 1,8-diisocyano-*p*-menthane)

Chi-Ming Che*, Hon-Kay Yip, Wing-Tak Wong and Ting-Fong Lai
Department of Chemistry, University of Hong Kong, Pokfulam Road (Hong Kong)

(Received November 20, 1991; revised April 29, 1992)

Abstract

The synthesis and X-ray crystal structures of [Au(ᵗBuNC)(CN)], [Au_2(dmb)$(CN)_2$] (dmb = 1,8-diisocyano-*p*-menthane) and [Au_2(tmb)$(CN)_2$] (tmb = 2,5-diisocyano-2,5-dimethylhexane) are described. [Au(ᵗBuNC)(CN)]: space group *Pnma*, $a = 13.437(1)$, $b = 6.469(1)$, $c = 9.823(1)$ Å, $Z = 4$, $R = 0.055$ for 673 observed Mo Kα data; [Au_2(dmb)$(CN)_2$]: space group $P2_1/c$, $a = 7.024(2)$, $b = 15.255(2)$, $c = 15.565(2)$ Å, $\beta = 101.33(2)$, $Z = 4$, $R = 0.050$ for 2137 observed Mo Kα data; [Au_2(tmb)$(CN)_2$]: space group *Pbcn*, $a = 15.629(3)$, $b = 9.222(4)$, $c = 22.777(3)$, $Z = 8$, $R = 0.036$ for 1127 Mo Kα data. The intermolecular Au...Au separations are 3.568, 3.49–3.73 and 3.21 Å for crystals of [Au(ᵗBuNC)(CN)], [Au_2(dmb)$(CN)_2$] and [Au_2(tmb)$(CN)_2$], respectively. $[Au_2(tmb)_2]^{2+}$ and $[Au_2(dmb)_2]^{2+}$ have also been synthesized by the reaction of Au(I) with the diisocyanide ligand. Their UV–Vis spectra are compared and discussed.

Introduction

The study of d^{10}–d^{10} metal interaction has been receiving close attention recently [1–3]. Interest in polynuclear d^{10} metal compounds also stems from their intriguing luminescent properties as reported by various groups [3–7]. It has been suggested that Au(I)–Au(I) interaction is responsible for the solid state photoluminescence of polymetallic gold(I) species [7–9]. Recently, we have communicated the X-ray crystal structure of [Au_2(dmb)$(CN)_2$] (dmb = 1,8-diisocyano-*p*-menthane) [6c]. Herein is described its detailed crystal structure and the structures of its related complexes [Au_2(tmb)$(CN)_2$] (tmb = 2,5-diisocyano-2,5-dimethylhexane) and [Au(ᵗBuNC)(CN)]. The dinuclear complexes $[Au_2(L)_2]^{2+}$ (L = tmb, dmb) have also been prepared and their UV–Vis absorption spectra are compared and discussed. Since the completion of this work, Harvey and co-workers have reported the X-ray structure of the related [Au_2(tmb)Cl_2] [9].

Experimental

Materials

Potassium tetrachloroaurate(III) and tert-butylisocyanide were obtained from Strem Co. Ltd. 2,2-Thiodiethanol and the starting materials for the synthesis of isocyanide ligands such as 1,8-diamino-*p*-menthane and 2,5-dimethyl-2,5-hexanediamine were purchased from Aldrich Chemicals. The ligands tmb and dmb were prepared according to the method reported by Weber *et al.* [10].

[Au(ᵗBuNC)(CN)] (1)

A methanolic solution of ᵗBuNC (0.6 g in 10 ml) was added dropwise with stirring to a methanolic solution of K[$AuCl_4$] (0.76 g in 10 ml). The yellow precipitate which initially formed gradually redissolved to a colorless solution together with some insoluble KCl. The reaction mixture was heated and stirred at 50 °C for 30 min and the KCl precipitate was filtered off. Upon evaporation of the filtrate down to 5 ml, white needle crystals of [Au(ᵗBuNC)(CN)] deposited (yield 59%). IR (nujol mulls) ν(CN): 2224, 2120 cm^{-1}.

[Au_2(dmb)$(CN)_2$] (2)

A mixture of dmb (0.6 g) and K[$AuCl_4$] (0.76 g) in methanol (25 ml) was stirred at room temperature. The yellow precipitate which formed was gradually redissolved upon heating the solution to 80 °C. The mixture became colorless and the insoluble KCl was removed by filtration. Colorless rod-like crystals (yield

*Author to whom correspondence should be addressed.

0020-1693/92/$5.00

49%) were obtained from the reaction mixture after two days. IR (nujol mulls), ν(CN): 2250, 2155 cm^{-1}.

$[Au_2(tmb)(CN)_2]$ (3)

A methanolic solution of tmb (0.6 g in 15 ml) was added in three separate portions with constant stirring to a methanolic solution of $K[AuCl_4]$ (0.76 g in 10 ml) at 50 °C. A pale blue solution with some white KCl solid was obtained after 50 min. This was filtered and the filtrate gave small colorless needle crystals upon standing (yield, 21%). IR (nujol mulls), ν(CN): 2250, 2160 cm^{-1}.

$[Au_2(L)_2](ClO_4)_2$ (L = tmb, dmb)

A methanolic solution of $K[AuCl_4]$ (0.3 g in 20 ml) was stirred with thiodiethanol (1 ml) for 15 min at room temperature. Excess isocyanide ligand L (dmb, 0.3: tmb, 0.25 g) was added to the solution which was continuously stirred until a clear colorless solution was obtained. Upon addition of $LiClO_4$, white solid $[Au_2(L)_2](ClO_4)_2$ was precipitated out. This was filtered and washed with deionized water and cold ethanol and air dried (yield 35–38%). *Anal.* Calc. for $[Au_2(dmb)_2](ClO_4)_2$: C, 29.6; H, 3.70; N, 5.75. Found: C, 29.4; H, 3.6; N, 5.60%. Calc. for $[Au_2(tmb)_2](ClO_4)_2$: C, 26.0; H, 3.47; N, 6.08. Found: C, 26.2; H, 3.60; N, 5.90%. IR (nujol mulls), ν(C≡N): 2260 cm^{-1} for both $[Au_2(tmb)_2](ClO_4)_2$ and $[Au_2(dmb)_2](ClO_4)_2$.

Physical measurements and instrumentation

UV–Vis spectra were obtained on a Shimadzu UV-240 spectrophotometer, steady-state corrected emission spectra on a Hitachi 650–60 fluorescence spectrophotometer. IR spectra were obtained as Nujol mulls on a Perkin-Elmer model 577 (4000–200 cm^{-1}) spectrophotometer.

X-ray crystal structure determination of 1, 2 and 3

X-ray diffraction data were collected on an Enraf-Nonius CAD4 diffractometer with graphite-monochromated Mo Kα radiation (λ = 0.71073 Å). Three checked reflections monitored every 2 h showed no intensity fluctuation for compounds **1** and **3**, but a loss of 11.4% in intensity was detected for compound **2** after 108 h of exposure and for which isotropic decay correction was applied. All intensity data were corrected for Lorentz, polarization and absorption effects; the empirical absorption correction was based on an azi-

TABLE 1. Crystal data and summary of data collection and refinement for compounds **1**, **2** and **3**

	Compound **1**	Compound **2**	Compound **3**
Formula	$Au(C_5H_9N)(CN)$	$Au_2(C_{12}H_{18}N_2)(CN)_2$	$Au_2(C_{10}H_{16}N_2)(CN)_2$
M	306.12	636.26	610.22
Space group	*Pnma*	$P2_1/c$	*Pbcn*
a (Å)	13.437(1)	7.024(2)	15.629(3)
b (Å)	6.469(1)	15.255(2)	9.222(4)
c (Å)	9.823(1)	15.565(2)	22.777(3)
β (°)		101.33(2)	
U (Å^3)	853.9	1635.3	3282.9
Z	4	4	8
F(000)	552	1152	2192
D_c (g cm^{-3})	2.381	2.584	2.469
D_m (g cm^{-3})	2.38	2.52	2.41
Crystal size (mm)	0.07×0.32×0.52	0.14×0.23×0.32	0.05×0.14×0.25
μ(Mo Kα) (cm^{-1})	171.3	178.4	178.2
Scan type, speed (° min^{-1})		ω–2θ, 1.1–5.5	
Scan width (°)		0.70 + 0.34 tanθ	
T (K)	295	298	295
Collection range, $2\theta_{max}$ (°)	50	52	45
Transmission factor	0.093–0.999	0.512–0.999	0.518–0.998
No. reflections measured	1745	6719	2469
No. unique data	912	3352	2469
No. data with $F_o > 3\sigma(F_o)$, m	673	2137	1127
No. parameters refined, p	53	182	163
R[a]	0.055	0.050	0.036
R[b]	0.068	0.059	0.039
S[c]	1.891	1.429	1.188
Residual extrema in final difference map (e Å^{-3})[d]	+3.20 to −2.95	+1.34 to −2.03	+0.625 to −0.748

[a] $R = \Sigma||F_o| - |F_c||/\Sigma|F_o|$. [b] $R' = [w(|F_o| - |F_c|)^2/\Sigma w|F_o|^2]^{1/2}$, with $w = 4F_o^2/[\sigma^2(F_o^2) + (0.04F_o^2)^2]$. [c] $S = [\Sigma w(|F_o| - |F_c|)^2/(m-p)]^{1/2}$. [d] Peaks are located in the neighbourhood of the Au atoms.

muthal (ψ) scan of reflections with χ close to 90°. The atomic scattering factors were taken from ref. 11. All computations were performed on a MICROVAX II computer using the Enraf-Nonius SDP programs [12].

The structures were solved by Patterson and Fourier methods and refined by full-matrix least-squares. All non-hydrogen atoms were generated geometrically and allowed to ride on their parent carbon atoms with fixed isotropic thermal parameters.

Crystal and structure determination data and final agreement factors are given in Table 1; atomic coordinates of non-hydrogen atoms in Tables 2, 3 and 4; selected bond distances and angles in Table 5.

TABLE 2. Fractional atomic coordinates for non-hydrogen atoms in compound **1** with e.s.d.s in parentheses

Atom	x	y	z
Au	0.52626(5)	0.250	0.43226(5)
N(1)	0.340(2)	0.250	0.249(1)
N(2)	0.729(1)	0.250	0.587(1)
C(1)	0.401(2)	0.250	0.322(2)
C(2)	0.649(2)	0.250	0.534(2)
C(3)	0.824(2)	0.250	0.655(2)
C(4)	0.803(2)	0.250	0.808(2)
C(5)	0.878(1)	0.058(3)	0.610(1)

TABLE 3. Fractional atomic coordinates for non-hydrogen atoms in compound **2** with e.s.d.s in parentheses

Atom	x	y	z
Au(1)	0.1045(1)	0.09546(4)	−0.06150(4)
Au(2)	0.3898(1)	−0.04871(4)	0.08888(4)
N(1)	0.100(2)	−0.0290(8)	−0.214(1)
N(2)	0.374(2)	−0.2059(9)	−0.0383(8)
N(3)	0.118(2)	0.2508(8)	0.0665(7)
N(4)	0.428(2)	0.0824(7)	0.2412(8)
C(1)	0.095(2)	0.0107(8)	−0.1558(8)
C(2)	0.383(2)	−0.1451(9)	0.0014(8)
C(3)	0.113(2)	0.192(1)	0.0230(8)
C(4)	0.413(2)	0.0375(8)	0.1855(9)
C(5)	0.118(2)	0.3272(8)	0.1299(8)
C(6)	0.010(5)	0.397(2)	0.073(2)
C(7)	0.336(3)	0.349(1)	0.164(1)
C(8)	0.447(2)	0.2709(9)	0.2115(8)
C(9)	0.372(3)	0.229(1)	0.281(1)
C(10)	0.453(3)	0.148(1)	0.3173(9)
C(11)	0.681(2)	0.160(2)	0.346(1)
C(12)	0.402(3)	0.109(1)	0.388(1)
C(13)	0.142(2)	0.215(1)	0.254(1)
C(14)	0.039(3)	0.292(1)	0.201(1)

TABLE 4. Fractional atomic coordinates for non-hydrogen atoms in compound **3** with e.s.d.s in parentheses

Atom	x	y	z
Au(1)	0.10457(4)	0.54559(9)	0.28055(3)
Au(2)	0.22794(5)	0.28268(9)	0.31771(4)
N(1)	0.133(1)	0.511(2)	0.1471(8)
N(2)	0.0968(8)	0.589(2)	0.4164(7)
N(11)	0.115(1)	0.130(3)	0.4101(8)
N(12)	0.3472(9)	0.431(1)	0.2283(7)
C(1)	0.119(1)	0.522(2)	0.1968(9)
C(2)	0.094(1)	0.573(2)	0.366(1)
C(3)	0.103(1)	0.605(3)	0.4794(7)
C(4)	0.017(1)	0.570(2)	0.507(1)
C(5)	0.118(3)	0.764(4)	0.488(1)
C(6)	0.174(2)	0.517(5)	0.498(1)
C(11)	0.155(1)	0.183(2)	0.3747(9)
C(12)	0.303(1)	0.377(2)	0.2624(8)
C(13)	0.411(1)	0.500(3)	0.190(1)
C(14)	0.496(2)	0.498(3)	0.218(1)
C(15)	0.379(2)	0.637(3)	0.166(1)
C(16)	0.414(2)	0.407(4)	0.139(2)

TABLE 5. Selected bond distances (Å) and angles (°)

Compound **1**			
Au–C(1)	2.00(2)	C(1)–N(1)	1.09(3)
Au–C(2)	1.93(3)	C(2)–N(2)	1.21(3)
C(1)–Au–C(2)	178.2(8)	Au–C(2)–N(2)	175(2)
Au–C(1)–N(1)	172(2)	C(2)–N(2)–C(3)	178(1)
Compound **2**			
Au(1)–C(1)	1.95(1)	Au(2)–C(2)	2.00(1)
Au(1)–C(3)	1.96(1)	Au(2)–C(4)	1.99(1)
N(1)–C(1)	1.10(2)	N(2)–C(2)	1.11(2)
N(3)–C(3)	1.12(2)	N(4)–C(4)	1.09(2)
N(3)–C(5)	1.53(2)	N(4)–C(10)	1.54(2)
C(1)–Au(1)–C(3)	173.2(5)	C(2)–Au(2)–C(4)	173.5(6)
Au(1)–C(1)–N(1)	171(1)	Au(2)–C(2)–N(2)	170(1)
Au(1)–C(3)–N(3)	176(1)	Au(2)–C(4)–N(4)	177(1)
Compound **3**			
Au(1)–C(1)	1.93(2)	Au(2)–C(11)	1.96(2)
Au(1)–C(2)	1.97(2)	Au(2)–C(12)	1.93(2)
N(1)–C(1)	1.15(3)	N(11)–C(11)	1.13(3)
N(2)–C(2)	1.16(3)	N(12)–C(12)	1.15(2)
N(2)–C(3)	1.44(3)	N(12)–C(13)	1.47(3)
C(1)–Au(1)–C(2)	177.7(7)	C(11)–Au(2)–C(12)	178.2(8)
Au(1)–C(1)–N(1)	177(2)	Au(2)–C(11)–N(11)	176(2)
Au(1)–C(2)–N(2)	173(1)	Au(2)–C(12)–N(12)	179(2)

Results and discussion

In the absence of 2,2′-thiodiethanol, the reaction of $AuCl_4^-$ with alkylisocyanide in alcohol led to dealkylation at the R–NC bond. Because of the electrophilic nature of Au(III), the coordinated isocyanide ligand undergoes rapid methanolysis.

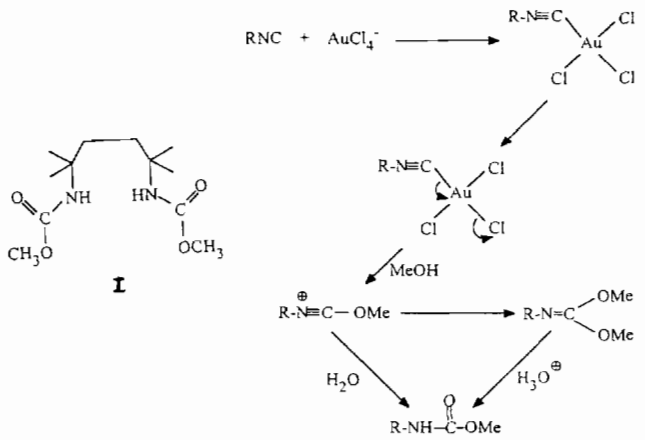

With R being a tertiary alkyl group, the formation of carbonium ion is also feasible and the dealkylation occurs as a competitive process.

$$[R\text{–}N{\equiv}C\text{–}AuCl_3] \longrightarrow [NC\text{–}AuCl_3]^- + R^+$$

The above scheme is supported by the isolation of the organic product **I** and $[Au_2(tmb)(CN)_2]$ from the reaction mixture of $AuCl_4^-$ and tmb in methanol. Compound **I** was characterized by X-ray crystallography [13], IR (ν(N–H), 3340 cm^{-1}; ν(C=O), 1700 cm^{-1}) and ^1H NMR spectroscopy. In the presence of 2,2'-thiodiethanol which acted as a reductant, Au(I) was formed *in situ*, which reacted with the bridging isocyanide ligand L giving $[Au_2(L)_2]^{2+}$. Although the X-ray structures of $[Au_2(L)_2]^{2+}$ have not been determined, their structures can be inferred from IR spectroscopy. Both $[Au_2(tmb)_2]^{2+}$ and $[Au_2(dmb)_2]^{2+}$ display only one single intense ν(C≡N) stretch at 2260 cm^{-1}, suggesting that the two bridging diisocyanide are *trans* to each other.

Structures

The monomeric [Au(^{t}BuNC)(CN)] (**1**) can be viewed as a prototype of interacting unit for $[Au_2(L)(CN)_2]$. Figure 1 shows the ORTEP diagram of **1**. The coordination geometry of the gold atom is almost linear with a C(2)–Au–C(1) angle of 178.2(8)°. The respective Au–C(CN) and Au–C(CN^{t}Bu) distances of 2.00(2) and 1.93(3) Å are nearly equal to those values found in the [Au(CH_3NC)(CN)] analogue whose structure has been reported previously [14]. Figure 2 shows the packing diagram of **1** viewed along the *c* axis. The crystal consists of rows of molecules parallel to the *a* axis and these molecules are weakly linked together via the gold atoms which form an infinite zig-zag chain parallel to the *b* axis with an Au–Au separation of 3.568 Å and Au–Au–Au angle of 130.1°. The crystal can then be viewed as a quasi-one-dimensional extended structure composed of monomeric [Au(^{t}BuNC)(CN)]. On the other hand, in the reported structure of [Au(CH_3NC)(CN)] [14], each gold atom is surrounded by six more distant gold atoms located approximately at corners of a regular hexagon and the gold atoms are linked weakly together into two-dimensional layers.

The structure of $[Au_2(dmb)(CN)_2]$ (**2**) has been briefly discussed in a previous communication [6c]. Remarkable features of this structure (Fig. 3) are the Au–Au distance of 3.54(1) Å which is considerably shorter than the

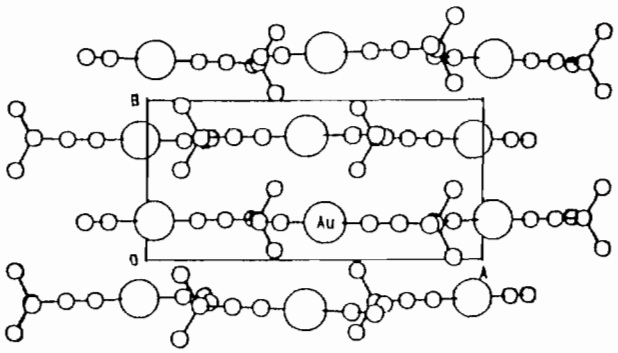

Fig. 2. Packing diagram of **1** viewed along the *c* axis.

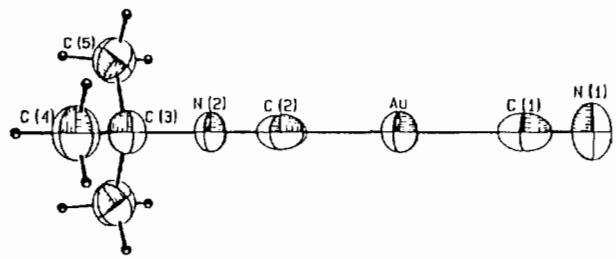

Fig. 1. ORTEP drawing of **1**. Thermal ellipsoids at 30% probability level.

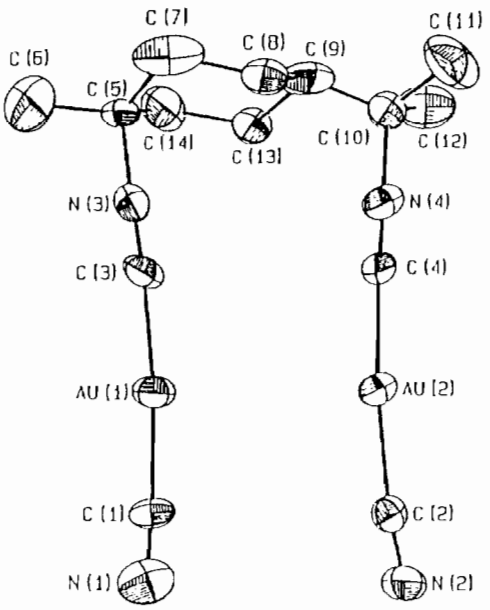

Fig. 3. ORTEP drawing of **2**. Thermal ellipsoids at 30% probability level.

bite distance (~4.45 Å) of the dmb ligand [15] and the deviation of the coordination of Au from perfect linearity (mean C–Au–C, 173.5(5)°). These findings suggest the possibility of there being a weak intramolecular bonding interaction. Interestingly, there are further intermolecular Au–Au contacts of 3.49 and 3.72 Å between adjacent pairs of $[Au_2(dmb)(CN)_2]$ molecules leading to an infinite inclined 'ladder' of golds atoms extended along the *a* axis as shown in Fig. 4. Note that one of the intermolecular Au–Au separations is 3.49 Å, which is even shorter than the intramolecular and intermolecular Au–Au separations found in $[Au(CH_3NC)(CN)]$ (3.52–3.72 Å) [14] and $K[Au(CN)_2]$ (3.63 Å) [8]. A similar ladder framework of gold atoms was found in $[(C_3H_7NH)Au(C{\equiv}C\text{–}Ph)]$ [16]. It is evident from Fig. 4 that each $[Au_2(dmb)(CN)_2]$ unit acts as a building block for a quasi-one-dimensional extended ladder structure.

It has been reported that complex **2** exhibits solid-state photoluminescence at room temperature. The luminescence, however, is similar to that observed in the $K[Au(CN)_2]$ [8] and $[Au_2(tmb)Cl_2]$ [9] solid. All these three complexes display high energy emission bands at similar energies: $K[Au(CN)_2]$, 390; $[Au_2(dmb)(CN)_2]$, 458; $[Au_2(tmb)Cl_2]$, 417 nm. The high energy emission of the $K[Au(CN)_2]$ solid has been argued to come from the two-dimensional Au–Au interactions [8]. Although the crystal packings of $[Au_2(dmb)(CN)_2]$ and $K[Au(CN)_2]$ are different from each other, the former has a even shorter interatomic Au–Au separation than the latter. It is therefore reasonable to argue that the high energy emission in **2** could also be assigned to come from states arising from Au–Au interactions.

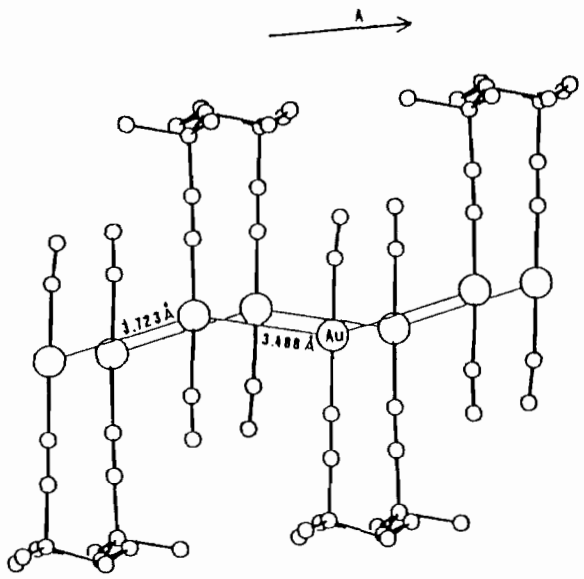

Fig. 4. Packing diagram of **2** showing an infinite inclined 'ladder' of gold atoms.

As a ligand, tmb is more floppy than dmb. For tmb, a single C–C bond rotation would lead to a conformational change from *syn* to *anti*. Observations of the *anti* conformation in metal–tmb complexes has recently been reported by Harvey and co-workers [9]. In this work, $[Au_2(tmb)(CN)_2]$ (**3**) has also been found to be more floppy and indeed two conformations are observed in the solid state. Figures 5 and 6 show the ORTEP drawings of the molecules. In one molecule the midpoint of the C(4)–C(4′) bond is located at a crystallographic inversion centre and in the others a crystallographic two-fold axis is perpendicular to the C(14)–C(14′) bond so that an asymmetric unit contains half of each of the two independent molecules. When looking through the C(4)–C(4′) or C(14)–C(14′) bond, the two independent $[Au_2(tmb)(CN)_2]$ molecules are both in *anti* conformation. The molecule can be considered as made up of two [^{t}BuNC–Au–CN] structural units linked together through one of the carbon atoms in the tert-butyl group. These two structural units are

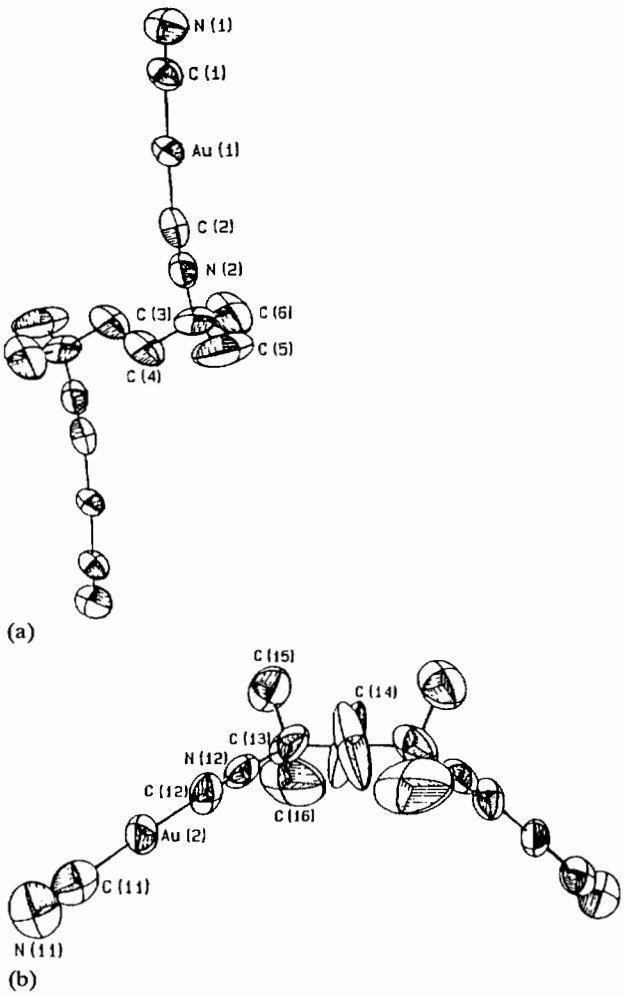

Fig. 5. ORTEP drawing of the two independent molecules in **3**: (a) with an inversion centre and (b) with a two-fold axis. Thermal ellipsoids at 30% probability level.

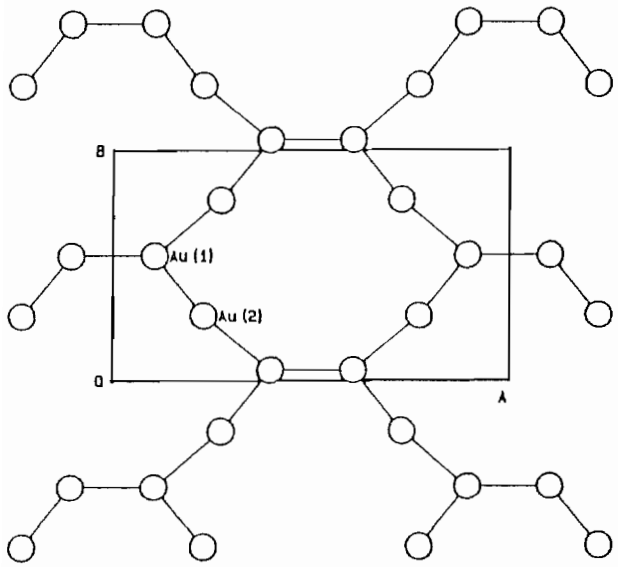

Fig. 6. View along the *c* axis showing a puckered layer of weakly linked Au atoms in **3**. The Au–Au distances range from 3.21 to 3.55 Å.

in *anti*-parallel conformation in Fig. 5(a) but subtend an angle of 126° in Fig. 5(b). In both molecules, the coordination geometry of the Au atoms is linear and the Au–C(CN) and Au–C(isocyanide) distances are virtually identical to those values found in **1** and **2**. The C–C distances and C–C–C angles in the tmb ligands are normal [9]. The shortest Au–Au contact found in the crystal of **3** is 3.21(2) Å, which is shorter than those found in complexes **1**, **2** and $[Au_2(tmb)Cl_2]$ [9].

The short Au–Au separation will lead to photoluminescence and as expected, a solid sample of **3** displays room temperature photoluminescence with similar emission energy ($\lambda_{max}^{emission} = 428$ nm) as that found in $[Au_2(tmb)Cl_2]$ [9]. Figure 6 shows that in the crystal of **3**, there are puckered layers of weakly linked Au atoms parallel to the *a*b* plane.

Spectroscopy of $[Au_2(L)_2]^{2+}$

Figure 7(a) and (b) show the room temperature electronic absorption spectra of acetonitrile solutions of $[Au_2(dmb)_2]^{2+}$ and $[Au_2(tmb)_2]^{2+}$, respectively. The spectrum for $[Au_2(dmb)_2]^{2+}$ is very similar to that reported for the mononuclear $[Au(EtNC)_2]^+$ [17]. Both complexes show an intense high energy absorption at 240–243 nm, which has been assigned to the ^{1}(MLCT) transition ($d_z^2 \rightarrow \pi^*$(RNC)) by Chastain and Mason [17]. The similarity in the electronic absorption spectra is not unexpected since the large bite distance of the dmb ligand would allow virtually no Au–Au interaction, thus offering only very small perturbation on the energy of the d_z^2 orbital. In $[Au_2(tmb)_{2+}]^{2+}$, the low energy allowed electronic transition is considerably red-shifted

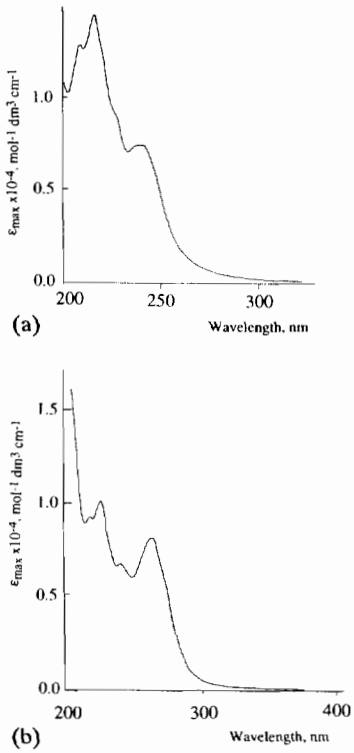

Fig. 7. UV–Vis absorption spectra of $[Au_2(dmb)_2]^{2+}$ and $[Au_2(tmb)_2]^{2+}$ in CH_3CN.

from $[Au_2(dmb)_2]^{2+}$ with an intense absorption band observed at 253 nm. We argue that this transition stems form Au–Au interaction because of the smaller bite distance of the tmb ligand. With reference to previous works [5b, 6a, 18] the 253 nm absorption band is assigned as the $d_\sigma^* \rightarrow p_\sigma$ transition where the p_σ orbital could have a substantial mixing with the π^* of the tmb ligand.

Supplementary material

Tables of H-atom coordinates, thermal parameters, bond distances and angles, and structure factors are available from the authors upon request.

Acknowledgements

We acknowledge support from the Croucher Foundation, the Hong Kong Research Grants Council and University of Hong Kong.

References

1 C. Kolmel and R. Ahlrichs, *J. Phys. Chem., 994* (1990) 5536.
2 (a) K. M. Merz, Jr. and R. Hoffmann, *Inorg. Chem., 27* (1988) 2120; (b) Y. Jiang, S. Alvarez and R. Hoffmann, *Inorg. Chem.,*

24 (1985) 749; (c) A. Dedieu and R. Hoffmann, *J. Am. Chem. Soc., 100* (1978) 2074; (d) P. K. Mehrotra and R. Hoffmann, *Inorg. Chem., 17* (1978) 2187.
3 F. A. Cotton, X. Feng, M. Matusz and R. Poli, *J. Am. Chem. Soc., 110* (1988) 7077.
4 (a) P. D. Harvey and H. B. Gray, *J. Am. Chem. Soc., 110* (1988) 2145; (b) P. D. Harvey, F. Adar and H. B. Gray, *J. Am. Chem. Soc., 111* (1989) 1312.
5 (a) N. I. Md. Khan, J. P. Fackler, Jr., C. King, J. C. Wang and S. Wang, *Inorg. Chem., 27* (1988) 1672; (b) C. King, J. C. Wang, N. I. Md Khan and J. P. Fackler, Jr., *Inorg. Chem., 28* (1989) 2145; (c) N. I. Md. Khan, C. King, D. D. Heinrich, J. P. Fackler, Jr. and L. C. Porter, *Inorg. Chem., 28* (1989) 2150; (d) S. Wang, G. Garzon, C. King, J. C. Wang and J. P. Fackler, Jr., *Inorg. Chem., 26* (1987) 4623.
6 (a) V. W. W. Yam, T. F. Lai and C. M. Che, *J. Chem. Soc., Dalton Trans.,* (1990) 3747; (b) C. M. Che, H. L. Kwong, C. K. Poon and V. W. W. Yam, *J. Chem. Soc., Dalton Trans.,* (1990) 3215; (c) C. M. Che, W. T. Wong, T. F. Lai and H. L. Kwong, *J. Chem. Soc., Chem. Commun.,* (1989) 243.
7 (a) A. Vogler and H. Kunkely, *Chem. Phys. Lett., 150* (1988) 135; (b) *158* (1989) 74; (c) K. R. Kyle, J. Dibenedetto and P. C. Ford, *J. Chem. Soc., Chem. Commun.,* (1989) 714; (d) H. Kunkely and A. Vogler, *Chem. Phys. Lett., 164* (1989) 621.
8 N. Nagasundaram, G. Roper, J. Biscoe, J. W. Chai, H. H. Patterson, N. Blom and A. Ludi, *Inorg. Chem., 25* (1986) 2947.
9 D. Perreault, M. Drouin, A. Michel and P. D. Harvey, *Inorg. Chem., 30* (1991) 2.
10 W. P. Weber, G. W. Gokel and I. K. Ugi, *Angew. Chem., Int. Ed. Engl., 11* (1972) 530.
11 *International Tables for X-Ray Crystallography*, Vol. 4, Kynoch, Birmingham, UK, 1974.
12 *Enraf-Nonius Structure Determination Packages,* SDP, Enraf-Nonius, Delft, Netherlands, 1985.
13 W. T. Wong, *M.Phil. Thesis,* University of Hong Kong, 1988.
14 S. Esperas, *Acta Chem. Scand., Ser. A, 30* (1976) 527.
15 (a) K. R. Mann, *Cryst. Struct. Commun., 10* (1981) 451; (b) C. M. Che, F. H. Herbstein, W. P. Schaefer, R. E. Marsh and H. B. Gray, *Inorg. Chem., 23* (1984) 2572.
16 P. W. R. Corfield and H. M. M. Shearer, *Acta Crystallogr., 23* (1967) 156.
17 S. K. Chastain and W. R. Mason, *Inorg. Chem., 21* (1982)3717.
18 (a) H.-R. C. Jarv, M. M. Savas, R. D. Rogers and W. R. Mason, *Inorg. Chem., 28* (1989) 1028; (b) W. Ludwig and W. Meyer, *Helv. Chim. Acta, 65* (1982) 934.